



# Gold nanoparticles embedded itaconic acid based hydrogels

M. Sakthivel<sup>1</sup> · D. S. Franklin<sup>2</sup> · S. Sudarsan<sup>3</sup> · G. Chitra<sup>3</sup> · T. B. Sridharan<sup>4</sup> · Guhanathan S.<sup>5</sup>

© Springer Nature Switzerland AG 2019

## Abstract

Traditional hydrogels have shown sub-standard multifunctional, mechanical properties in biomedical field. Gold nanoparticles can provided an expanded array of nanostructured materials with exclusive biomedical properties. The nanocomposite hydrogels have expected to exhibit both nanomaterial and hydrogel properties, which may resulted in potential applications in biomedical field. Hence, the present investigation reported simple and greener approach to the preparation and properties of pH-responsive nanocomposite hydrogels (GIAE) based on itaconic acid (IA), acrylic acid, ethylene glycol and colloidal gold nanoparticles. The obtained nanocomposite hydrogels found to have desired exfoliated surface morphology and enhanced pH-sensitive swelling and thermal stability. It also showed appreciable anti-microbial properties due to presence of gold nanoparticles and IA. The cytotoxicity nature of itaconic acid based gold nanocomposite hydrogels were also developed ~ 90% due gold nanoparticles. Moreover, the degradation property of prepared nanocomposite hydrogels have been reduced due to bacterial inhibition tendency of gold nanoparticles. This work provides viewpoints to develop pH-tunable GIAE nanocomposite hydrogels with significant biological properties. The resultant nanocomposite hydrogels may be recommended for biomedical applications mere in future such as pH-sensitive drug delivery, scaffold for tissue engineering, wound healing application, antimicrobial material and nanomedicine etc.

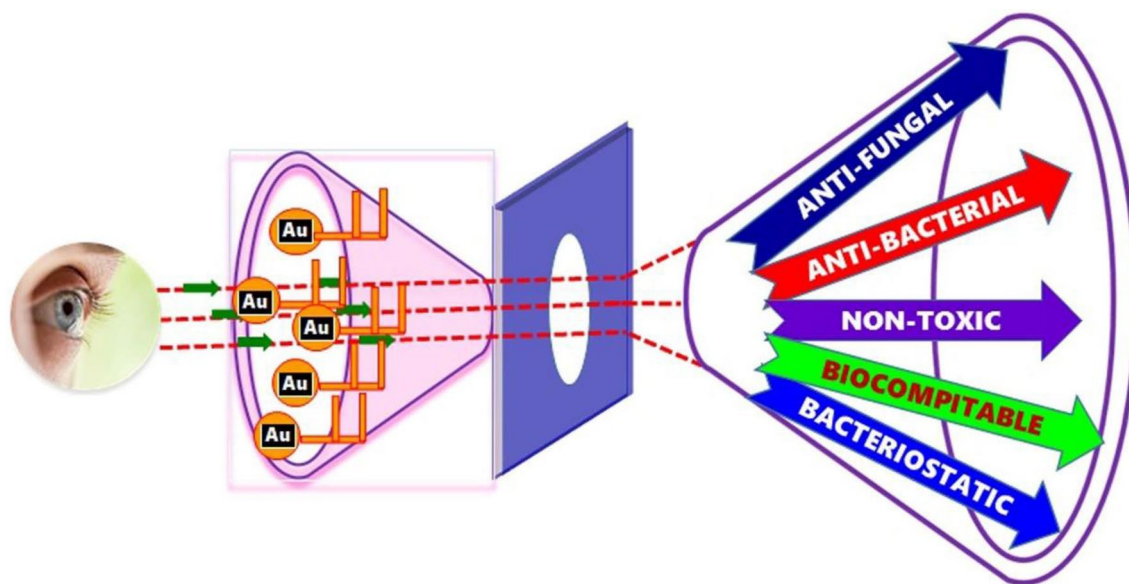
✉ GuhanathanS., sai\_gugan@yahoo.com; M. Sakthivel, msakthi81986@gmail.com; D. S. Franklin, loyolafrank@yahoo.co.in; S. Sudarsan, srsudarsan29@gmail.com; G. Chitra, chitramuralikrishnan@gmail.com; T. B. Sridharan, tbsridharan@vit.ac.in | <sup>1</sup>Research and Development Centre, Bharathiar University, Coimbatore, Tamilnadu 641 046, India. <sup>2</sup>Department of Chemistry, C. Abdul Hakeem College of Engineering and Technology, Melvisharam 632 509, India. <sup>3</sup>Department of Chemistry, Periyar University, Salem, Tamilnadu 636 011, India. <sup>4</sup>School of Biosciences and Technology, VIT University, Vellore 632 014, India. <sup>5</sup>PG & Research Department of Chemistry, Muthurangam Government Arts College, Vellore, Tamilnadu 632 002, India.

SN Applied Sciences (2019) 1:146 | <https://doi.org/10.1007/s42452-018-0156-y>

Received: 15 November 2018 / Accepted: 28 December 2018

Published online: 03 January 2019

## Graphical abstract



**Keywords** Itaconic acid · Acrylic acid · Anti-microbial behaviour · pH-sensitiveness · Biocompatible

## 1 Introduction

The nanocomposite hydrogels have shown great attention in biomedical field due to their distinctive properties such as, swelling capability, biocompatibility and anti-microbial nature [1]. The ability to absorb aqueous solutions make them an exclusive material for various biomedical applications such as, contact lenses, artificial corneas, burn dressing, food industry, water purification and separation process [2]. The nanocomposite hydrogels have also shows great application in the pharmaceutical field and especially in drug delivery applications [3]. Among them, itaconic acid based hydrogels are quite important due to their versatile use in many biomedical applications which similar to any other hydrogels. Since, the unsaturated itaconic acid has chosen to prepare a new variety of pH-sensitive gold nanocomposite hydrogels. In general, itaconic acid possesses two carboxylic moieties in one molecule which achieves the pH-sensitiveness of hydrogels. In general, natural monomer-based nanocomposite hydrogels are biodegradable, highly hydrophilic and they possess good biomedical properties [4]. Besides, itaconic acid provides its outstanding assets in polymer chemistry, pharmaceutical, and agricultural applications [5].

The incipient applications of hydrogels have developed particularly for cancer research [6]. Demand in biomedical applications, the biomedical materials must possess multiple functionalities [7]. Hence, the present investigation

focused to synthesized itaconic acid based, gold nanoparticles embedded hydrogels with multifunctional in nature. A range of nanoparticles such as gold, silver and iron oxide is binding with polymeric hydrogels to obtain nanocomposite hydrogels viz. physical, chemical interaction providing unique properties to nanocomposite hydrogels [8]. Developing nanocomposite hydrogels with tailored functionalities have possibilities to improve a biomaterial in various biomedical and biotechnological applications [9].

The modification of surface interaction between the nanoparticles and polymeric chain may leads to change in material properties resulting in useful biomedical applications. Conversely, many nanocomposite hydrogels lack in some important features such as stimuli sensitive, biodegradation and biocompatible properties [10]. Hence, the present investigation focused on pH-sensitive nanocomposite hydrogels. Thomas et al. [11] have been reported nano particles such as silver, gold, and copper is highly toxic to microorganisms due to their strong biocidal effects. Bal1 et al. [12] have prepared itaconic acid based silver nanocomposite hydrogels with a lesser swelling ratio due to  $\text{Ag}^+$  complexation with carboxyl moieties. Tibbitt et al. [13], reported that for stem cell engineering, immunomodulation and cancer research applications demand multiple functionalities of the hydrogel network and dynamic interactions between the surrounding cells. Infections associated with medical implants are becoming increasingly common and result in significant

morbidity and, in some cases, loss of natality [14]. Thus the synthesis of hydrogels with bactericidal properties has been interested. Another promising approach is the addition of metal nanoparticles as alternative to antibiotics because of the increasing bacteria population exhibiting resistance to these drugs consequently reducing their applicability [15]. Silver nanoparticles have been shown effective to combat bacteria, viruses and eukaryotic microorganisms [16]. Besides, gold nanoparticles makes hydrogels suited for medical purposes. Biodegradable hydrogels have achieved attention towards many researchers due to their activity for biological interaction with human body cells. Henceforth, they can be utilized in biomedical applications [17]. Jayaramudu et al. 2013 have prepared degradable gold nanocomposite hydrogels viz. enzymatic degradation under controlled condition. In contrary to that, the prepared nanocomposite hydrogels have also underwent for biodegradation in a natural environment without any external assistance [18]. In general, gold nanocomposite hydrogels have shown great attention among the researchers for their valuable application as an antimicrobial material [19].

The scope of the present investigation to delineate the good itaconic acid based biomaterial by green perception with multiple functionality. The obtained hydrogels have interpreted in depth with FT-IR, SEM, TEM, EDX, UV, TGA, DTA, pH-stimuli, anti-microbial, cytotoxicity and biodegradation studies. In order to investigate as biomaterial, the resultant itaconic acid based gold nanocomposite hydrogels subjected to various pathogens. In conclusion, the results of antimicrobial studies were parallel to the positive control. The thermal stability of gold nanocomposite hydrogels has been raised upon the stoichiometric concentration of gold nano particles. The prepared gold nanocomposite hydrogels can be useful for pH-sensitive drug delivery, scaffold for tissue engineering, wound healing application, antimicrobial material, switchable electronics, intelligent therapeutic system and nanomedicine etc. Herein, the study of preparation of GIAE gold nanocomposite hydrogels for significant biomaterial is presented.

## 2 Experimental

### 2.1 Materials

Acrylic acid (AA) and Ethylene glycol (EG) and were received from Merck chemicals (Mumbai, India). Itaconic acid (IA) was obtained from Sigma Aldrich chemicals (Bangalore, India). AA was vacuum distilled at 54 °C/25 mm Hg to remove the inhibitor hydroquinone. Potassium per sulphate ( $K_2S_2O_8$ ) and *N,N'*-Methylene bis-acrylamide were obtained from Sigma Aldrich chemicals (Bangalore, India).

Double distilled water used for polymerizations and preparation of buffer solutions.

### 2.2 Preparation of Gold nanoparticles

The gold nano particles were obtained by citrate reduction method. 300 mL of 0.5 mm  $H AuCl_4$  was boiled with 30 mL of 38.8 mm trisodium citrate by vigorous stirring until the temperature reach at 97 °C. The resulting pale yellow colour was turned into brilliant red colour. The obtained colloidal gold nano solution was stored in amber bottle at room temperature.

### 2.3 Preparation of gold nanocomposite hydrogels GIAE

The pH-sensitive GIAE nanocomposite hydrogels of various compositions were carried out by radical polymerization viz. green perception according to the modified procedure, reported previously [20]. Initially the itaconic acid was dissolved in distilled water. Followed by ethylene glycol was added into polymerization tube. The polymerization was carried out at 75 °C for 30 min with continuous stirring in an inert nitrogen atmosphere. The obtained intermediate labelled as a pre-polyester. Furthermore, the initiator  $K_2S_2O_8$  (0.05 g) and *N,N'*-Methylene bis-acrylamide (0.05 g) cross linker were also added along with a stoichiometric amount of acrylic acid and the gold nano colloidal solution. The free radical polymerization was continued at 75 °C for 1.30 h. The formed pale brown gel confirmed the completion of radical polymerization. The final product was named as GIAE nanocomposite hydrogel. Conversely, the obtained product was immersed in distilled water for a week to remove any unreacted chemicals, by changing water daily and then dried at room temperature. Various compositions of GIAE nanocomposite hydrogels have been prepared by changing the stoichiometry of itaconic acid, ethylene glycol and colloidal gold nano solution. The notation, description of GIAE nanocomposite hydrogels have been shown in Table 1.

### 2.4 FT-IR spectroscopic studies

Nanocomposite hydrogels (1 g/L) were crushed into a powder and mixed with KBr pellets. The FT-IR studies were carried out at room temperature. The spectra recorded over the wavelength range of 400–4000 with a resolution of  $2\text{ cm}^{-1}$  using an Alpha Bruker-2009 spectrophotometer.

### 2.5 Scanning electron microscopy (SEM)

A SEM (JSM-6701S) was used to identify the specimen morphology of GIAE nanocomposite hydrogels. The

**Table 1** Stoichiometric quantities and physical exterior of GIAE nanocomposite hydrogels based on IA, EG, AA and Au-NANO solution and distilled water

S. no	Sample	Composition (mole)			Au-nano solution (mL)	Distilled water (mL)	Description
		IA	AA	EG			
1	G <sub>1</sub> I <sub>1</sub> A <sub>1</sub> EG <sub>1</sub>	0.01	0.025	0.01	0.1	10.0	No gel formation
2	G <sub>1</sub> I <sub>1</sub> A <sub>1</sub> EG <sub>4</sub>	0.01	0.025	0.04	0.5	10.0	Pale brown, insoluble in water
3	G <sub>2</sub> I <sub>2</sub> A <sub>1</sub> EG <sub>3</sub>	0.02	0.025	0.03	1.0	10.0	Pale brown, insoluble in water
4	G <sub>3</sub> I <sub>2</sub> A <sub>1</sub> EG <sub>2</sub>	0.03	0.025	0.02	1.5	10.0	Pale brown, insoluble in water

swollen samples were freeze dried and kept in a vacuum. The prepared hydrogels were silver sputter coated under vacuum before observation. All the experiments were performed in triplicate.

## 2.6 pH-sensitive swelling studies

Dynamic swelling experiments were performed in 50 ml of prepared carbonate buffer solutions (CBS) in a flask of desire pH values ranging from 1.2. to 10.0 at ambient temperature. The swollen nanocomposite hydrogels were removed from swelling medium at regular intervals. Followed by gels were dried superficially with clean tissue paper, weighed and replaced in the same flask. The swelling measurements were continued until constant weight was reached for each sample. The amount of water uptake was monitored gravimetrically. The needed pH of a buffer medium was attained through 0.01 M dil HCl and 0.01 M dil NaOH. The pH of buffer medium was checked by the pH meter (Citizen 3000). The degree of swelling equilibrium ( $S_{eq}$  %) was calculated as follows Eq. (1).

$$S_{eq} \% = \frac{W_{eq} - W_d}{W_d} \times 100 \quad (1)$$

Here,  $W_d$  is the initial weight of dried hydrogel,  $W_t$  is the weight of the swollen hydrogel at regular time interval  $t$ ,  $W_{eq}$  weight of the swollen sample at equilibrium. All the swelling experiments were performed in triplicate.

## 2.7 Thermal analysis

The decomposition temperature of itaconic acid based gold nanocomposite hydrogels were assessed by using the Thermo Gravimetric Analyser (TGA) using SEIKO model TG/DTA 6200.U system, in the temperature range from 20 to 8000 °C at the flow rate of 100 °C/min, under a dynamic N<sub>2</sub> atmosphere.

## 2.8 UV-visible spectroscopy

Freeze dried gold nanocomposite hydrogels were directly analysed by using UV-visible spectroscopy, i.e., LABINDIA

model UV 320 at room temperature. The itaconic acid based gold nanocomposite hydrogels were recorded in the absorbance range of 200–700 nm.

## 2.9 Energy-dispersive X-ray (EDX) spectroscopy

Energy-dispersive X-ray (EDX) spectroscopy is an analytical technique used for the elemental analysis or chemical characterization of gold nanocomposite hydrogel samples using Philips XL30 model, × 15–× 200,000 magnification with 2 nm resolution.

## 2.10 Transmission electron microscopy (TEM) analysis

Transmission Electron Microscope (TEM) utilized to provide morphological, compositional information of gold nanocomposite hydrogels using LaB6 JEM 2000 model, 2000 ×–1,500,000 × magnification with 0.23 nm resolution.

## 2.11 In vitro antibacterial activity assay

The virgin nanocomposite hydrogel (antibiotic unloaded) samples were inoculated in tubes with sterile saline solution (3 ml) at 37° C for 24 h. The selected indicator microorganisms were *Staphylococcus aureus* (MTCC430), *Bacillus cereus* (MTCC3311) and *Escherichia coli* (MTCC739). The assay was conducted in Nutrient Agar (NA) plates seeded which seeded broth culture of different bacteria for 8 h. In each of these plates were cut out using sterile cork borer. The samples were cautiously added with different concentrations (150, 300, 450 and 600 µg) into wells by using sterilized dropping pipette. Followed by, the wells were permitted to diffuse at room temperature for 2 h, later the plates were incubated in a sealed container at 37 °C for 18–24 h. The *Gentamicin* (500 µg) was elected as a positive control and distilled water was used as negative control. The antimicrobial activity of GIAE nanocomposite hydrogels was assessed by measuring the diameter of inhibition zone.

## 2.12 Anti-fungal assay

Antifungal activity of virgin (antibiotic unloaded) GIAE nanocomposite hydrogels were tested using the well diffusion method. Petri plates were prepared with 20 ml of sterile MHA (Hi-media, Mumbai). The test culture was swabbed on the top of solidified media and allowed to dry for 10 min. Wells were made in the media using a well borer. The various concentrations of the sample (15, 30, 45 and 60  $\mu\text{l}$  per well) were loaded on the wells. Ketakonazole (100  $\mu\text{g}$ /well) used as a positive control. These plates were incubated at 28 °C for 48 h in closed condition. The zone of inhibition was noticed in millimeters (mm).

## 2.13 In vitro cytotoxicity studies

The Cytotoxicity is being able to cause damage or death of normal cells. In order to identify the cell proliferation of GIAE nanocomposite hydrogels, the 3T3 fibroblast cell lines were plated separately in 96 well plates at a concentration of  $1 \times 10^5$  cells/well. After 24 h cells washed thrice with 100  $\mu\text{l}$  of serum-free medium and starved at 37 °C for 1 h. Subsequently, after starvation, cells were treated with the test compound for 24 h and 72 h. At the end of the treatment the medium was aspirated and serum free medium containing 3-(4,5-Dimethylthiazol-2-Yl)-2,5-Diphenyltetrazolium Bromide (MTT) (0.5 mg/ml) was added and incubated for at 37 °C in for 4 h in a CO<sub>2</sub> incubator.

The (3-(4,5-Dimethylthiazol-2-Yl)-2,5-Diphenyltetrazolium Bromide (MTT) holding medium was then discarded and the cells were washed with phosphate buffered saline (PBS) (200  $\mu\text{l}$ ). The crystals were then dissolved by adding 100  $\mu\text{l}$  of DMSO and it was mixed properly by pipetting up and down. Spectrophotometrically absorbance of the purple, blue formazan dye was measured in a microplate reader at 570 nm (Biorad 680). Cytotoxicity was determined using Graph pad prism-5 software.

## 2.14 Soil buried biodegradability

Biodegradable is one among the special advantage of hydrogels. Biodegradation in which substances are decomposed by aerobic bacteria into simpler substances such as carbon dioxide and water etc. Biodegradation of the GIAE nanocomposite hydrogels was carried out under natural environment condition for 90 days. A 0.5 gm of GIAE nanocomposite hydrogel was buried in soil with a sealed tip tea bag which are commonly made up of filter paper, silk etc. The relative humidity was maintained at 65%. Followed by, every 15 days once partially degrade hydrogel removed from soil and washed well with fresh water to avoid environmental impurities. Then, it was placed in a vacuum for 8 h at 37 °C until it gets constant

weight. Once the weighing completed, the GIAE hydrogel replaced in the same place. Degrade weight of nanocomposite hydrogels was calculated by weight loss method using following formula (2).

$$\text{Weight loss} = \frac{M_{t1} - M_{t2}}{M_{t1}} \times 100 \quad (2)$$

where  $M_{t1}$  is pre weight of dried hydrogel and  $M_{t2}$  is post weight of degrade hydrogel at each time intervals.

## 3 Results and discussion

### 3.1 FT-IR spectral studies of GIAE gold nanocomposite hydrogels

The conformation of gold nanocomposite hydrogels networks have investigated by FT-IR spectroscopic analysis Fig. 1. The  $G_1I_1A_1EG_4$  (Fig. 1b) nanocomposite hydrogel observed a broad peak at  $3420 \text{ cm}^{-1}$  might be to hydrogen

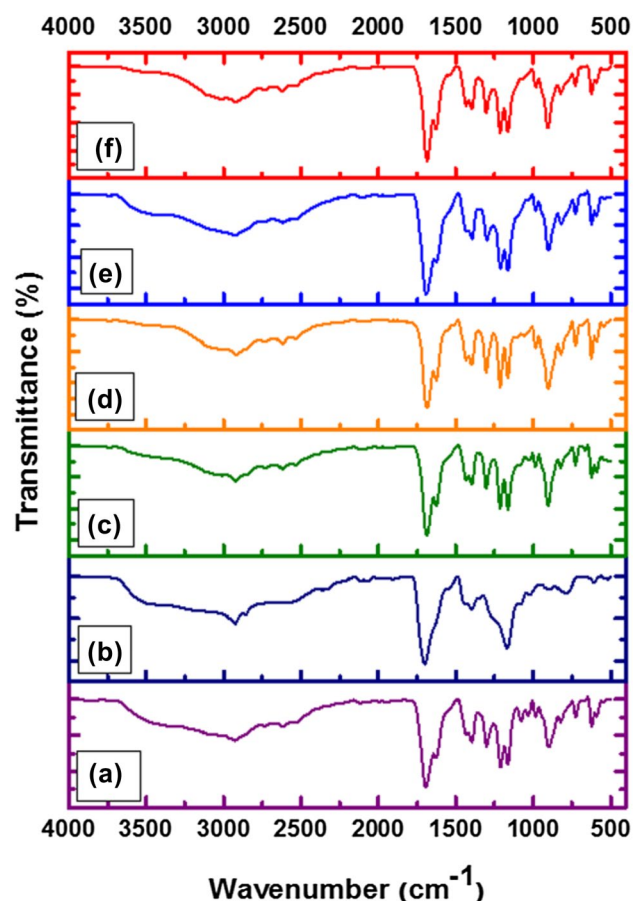


Fig. 1 Comparative FT-IR spectra of polymeric  $I_1A_1EG_4$  (a),  $I_2A_1EG_3$  (c),  $I_3A_1EG_2$  (e) and gold nanocomposite hydrogels  $G_1I_1A_1EG_4$  (b),  $G_2I_2A_1EG_3$  (d),  $G_3I_3A_1EG_2$  (f)

bonded OH stretching frequency. It is found that a characteristic absorption peak at  $2917\text{ cm}^{-1}$  corresponding to aliphatic  $\text{CH}_2$  stretching. The FT-IR spectrum of C=O occurred at  $1696\text{ cm}^{-1}$  (Fig. 1a) for a polymeric hydrogel while, it shifted to higher wave number  $1687\text{ cm}^{-1}$  associated with the C=O stretching frequency in nanocomposite hydrogel [21]. It indicated that complexation took place in between the  $\text{COO}^-$  and Au nanoparticles. Similarly, the  $\text{G}_2\text{I}_2\text{A}_1\text{EG}_3$  nanocomposite hydrogel the C=O stretching frequency shifted to lower frequency at  $1679\text{ cm}^{-1}$  (Fig. 1d) Likewise,  $\text{G}_3\text{I}_3\text{A}_1\text{EG}_2$  gold nanocomposite hydrogel has also showed shifted wavenumber at  $1678\text{ cm}^{-1}$  (Fig. 1f). The broad vibration at  $3396, 3408\text{ cm}^{-1}$  characteristic to O–H of  $\text{G}_2\text{I}_2\text{A}_1\text{EG}_3$  and  $\text{G}_3\text{I}_3\text{A}_1\text{EG}_2$  gold nanocomposite hydrogels. C–H symmetrical and asymmetrical stretching at  $2920\text{ cm}^{-1}$  and  $2917\text{ cm}^{-1}$  with respect to  $\text{G}_2\text{I}_2\text{A}_1\text{EG}_3$  and  $\text{G}_3\text{I}_3\text{A}_1\text{EG}_2$  gold nanocomposite hydrogels. Many peaks appeared in the range of  $1500\text{--}700\text{ cm}^{-1}$  due presence of CH,  $\text{CH}_2$ , and C–C and C–O groups of prepared nanocomposite hydrogels [22]. Therefore, the FT-IR spectroscopy analysis revealed that concrete evidence for mode of binding of Au nanoparticles with polymeric backbone [23].

### 3.2 Morphological studies of GIAE gold nanocomposite hydrogels

The Scanning electron microscope (SEM) is the most widely used for investigation of the shape, size, morphology, and porosity of hydrogel matrices. The morphology of the GIAE nano composite hydrogels were examined by SEM analysis, shown in Fig. 2. Micrograph for  $\text{G}_1\text{I}_1\text{A}_1\text{EG}_4$  nanocomposite hydrogel (a, b) revealed that needle and dent like homogeneous surface morphology. It also exhibits the smaller gold nanoparticles distributed throughout the hydrogel matrix. The  $\text{G}_2\text{I}_2\text{A}_1\text{EG}_3$  (c, d) nanocomposite hydrogel showed rough surface morphology along with the presence of spherical gold nanoparticles. The  $\text{G}_3\text{I}_3\text{A}_1\text{EG}_2$  (e, f) nanocomposite hydrogel showed pitting surface morphology. In general, the gold nanoparticles are prone to aggregate with hydrogel matrix due to large surface area [24]. The smooth and porous structure of GIAE nanocomposite hydrogels showed that expected to work as a unified biomedical system. Moreover, the morphology represents the GIAE nanocomposite hydrogels were exhibited the small uneven cavities, which encourage the swelling nature of hydrogels. The porous morphology of GIAE nanocomposite hydrogels were mainly due to concentration of itaconic acid and gold nanoparticles respectively.

### 3.3 Equilibrium swelling studies of GIAE gold nanocomposite hydrogels

The comparative equilibrium swelling behavior of GIAE nanocomposite hydrogels were carried in pH medium in between 1.2 and 10.0. The equilibrium swelling results have shown in Fig. 3. According to swelling equilibrium results of GIAE nanocomposite hydrogels showed gradual increase in swelling behaviour in the presence of acidic to basic buffer medium. The prepared nanocomposite hydrogels have showed a maximum of swelling at pH 10.0 due to anion–anion repulsive force as well as complete dissociation of carboxylate moieties. Meanwhile, at lower pH due to protonation of carboxylate groups, nanocomposite hydrogels shrink within a network. The  $\text{G}_1\text{I}_1\text{A}_1\text{EG}_4$  nanocomposite hydrogel exhibited 1740% and  $\text{G}_2\text{I}_2\text{A}_1\text{EG}_3$  revealed 2260% and  $\text{G}_3\text{I}_3\text{A}_1\text{EG}_2$  shown 2800% of swelling in 24 h. As the concentration of itaconic acid and gold nanoparticles increases, the swelling behavior also increased. It is due to additional osmotic pressure develops that expands the gel network further [25]. Swelling behavior of GIAE nanocomposite hydrogels makes them appropriate candidates for controlled drug delivery systems. In general, addition of gold nanoparticles within the hydrogel, expands the gel networks and promotes higher water uptake capacity [26].

### 3.4 TGA-DTA studies of GIAE gold nanocomposite hydrogels

The TGA and DTA thermogram of  $\text{G}_1\text{I}_1\text{A}_1\text{EG}_4$  nanocomposite hydrogel have shown in Fig. 4. The  $\text{G}_1\text{I}_1\text{A}_1\text{EG}_4$  nanocomposite hydrogels observed three stages of decomposition. The first weight loss (18.6%) step occurring over the range  $40\text{--}188\text{ }^\circ\text{C}$  may be attributed to the loss of residual water. The main stage of decomposition occurred from  $248\text{ to }351\text{ }^\circ\text{C}$  with weight loss of 47.3%. It is due to hydrogel in the case of crosslinked polymers suggested oxidative decomposition. The third stage decomposition started from  $410\text{ to }528\text{ }^\circ\text{C}$  with weight loss of 79%. It might be to de-polymerization of  $\text{G}_1\text{I}_1\text{A}_1\text{EG}_4$  nanocomposite hydrogel. Similarly, the Fig. 5 shows TGA–DTA thermogram of  $\text{G}_2\text{I}_2\text{A}_1\text{EG}_3$  nanocomposite hydrogel. The thermogram of  $\text{G}_2\text{I}_2\text{A}_1\text{EG}_2$  nanocomposite hydrogel showed three decomposition stages. The first decomposition stage in the range  $40\text{--}199\text{ }^\circ\text{C}$  with weight loss of 19%, which attributed to the loss of bounded water. The second one in the interval of  $277\text{--}374\text{ }^\circ\text{C}$  and the weight loss had been 51%. It has been described to decarboxylation of the polymeric nanocomposite which leads to the formation of inter- and intra-molecular anhydride. The third decomposition was in the range of  $417\text{--}554\text{ }^\circ\text{C}$  with weight loss of

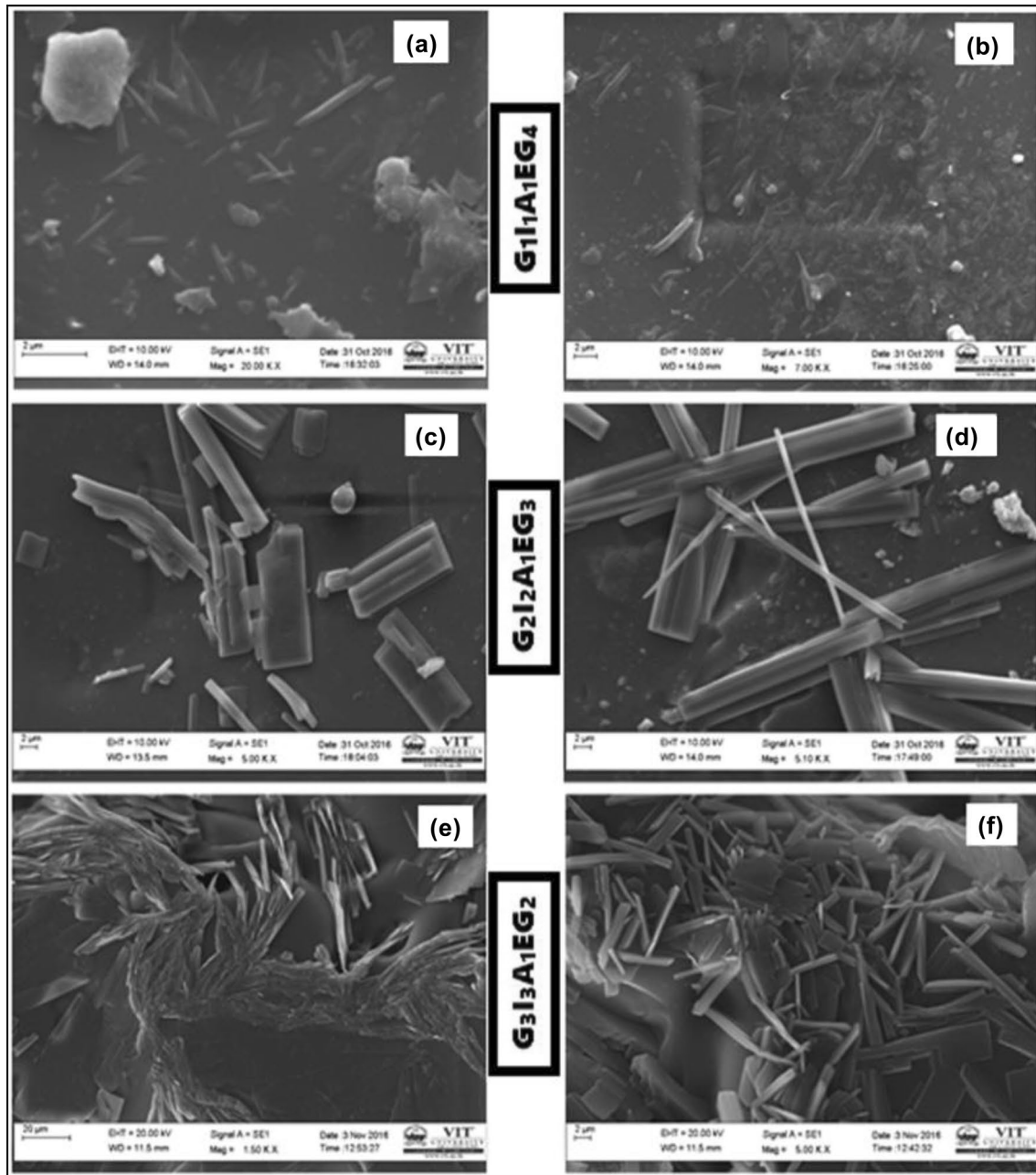


**Fig. 2** SEM images of  $G_{1I_1A_1EG_4}$  (**a, b**)  $G_{2I_2A_1EG_3}$  (**c, d**) and  $G_{3I_3A_1EG_2}$  (**e, f**) nanocomposite hydrogels

80%. It is due to degradation of the residual polymer. The Fig. 6 exhibited the TGA & DTA thermogram of  $G_{3I_3A_1EG_2}$  nanocomposite hydrogel. The first degradation temperature between 40 and 205 °C with weight loss of 20%, which due to easily bounded water. The second stage decomposition at 268–374 °C with 49% of weight loss. It is attributed to loss of crosslinking of polymeric matrix. The final decomposition noticed at 422–580 °C with a loss of 81%. The DTA results of GIAE nanocomposite

hydrogels were also well supported by TGA results with necessary exothermic and endothermic peaks. Moreover, the thermal results of  $G_{3I_3A_1EG_2}$  nanocomposite hydrogels were significantly higher thermal stability than the  $G_{1I_1A_1EG_4}$ ,  $G_{2I_2A_1EG_2}$  nanocomposite hydrogels. This study indicates, the improvement of thermal stability of nanocomposite hydrogels might be to the “nano-effect” of gold particles [27].

**Fig. 3** Comparative swelling equilibrium percentage of  $G_{11}A_1EG_4$ ,  $G_{21}A_1EG_3$  and  $G_{31}A_1EG_2$  nanocomposite hydrogels with various pH 1.2, 6.0, 7.4 and 10.0

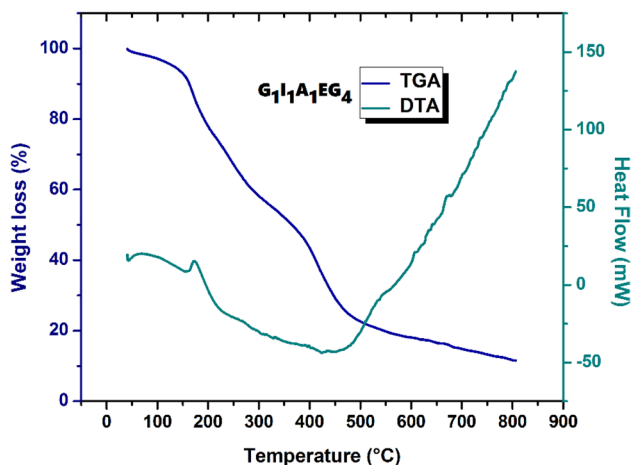
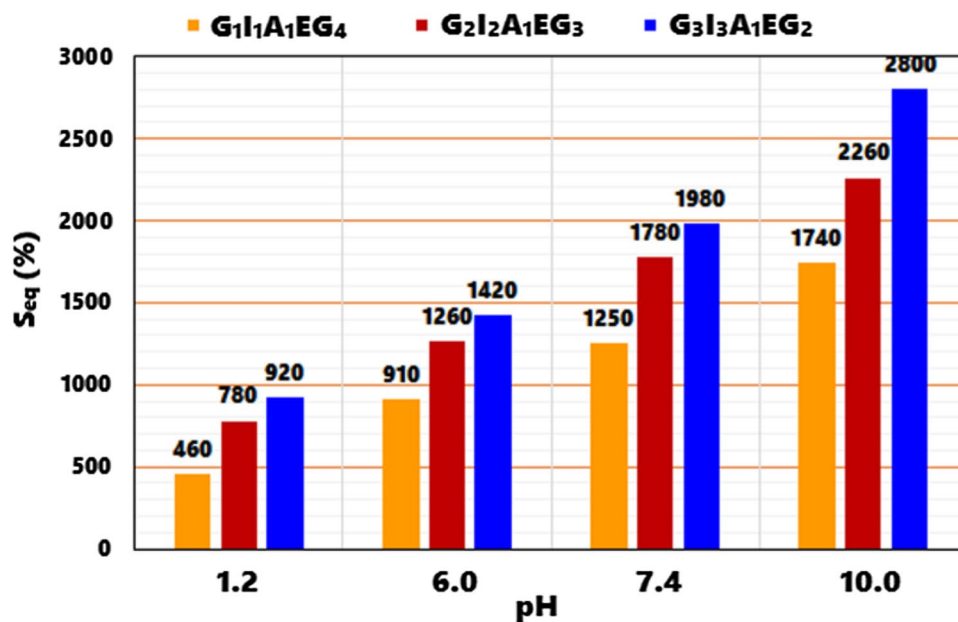


**Fig. 4** TGA–DTA thermogram of  $G_{11}A_1EG_4$  nanocomposite hydrogel

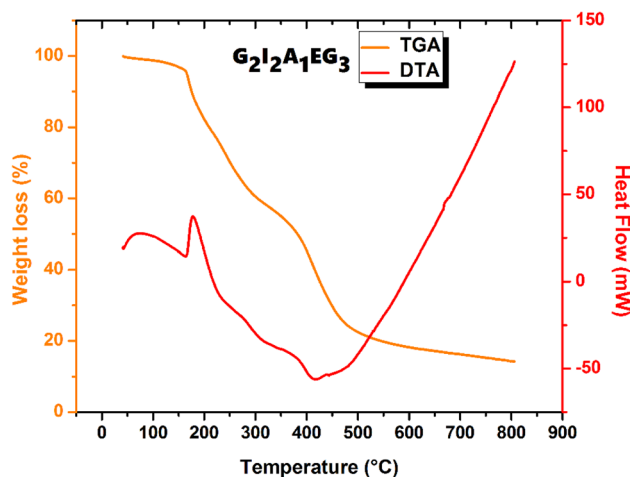


**Fig. 5** TGA–DTA thermogram of  $G_{21}A_1EG_3$  nanocomposite hydrogel

### 3.5 UV-spectral studies of GIAE gold nanocomposite hydrogels

The UV–vis spectra of gold nanoparticles incorporated GIAE nanocomposite hydrogels shown in Fig. 7. The GIAE nanocomposite hydrogels showed a distinct characteristic absorption peak around 530 nm. This must be due to the characteristic surface plasmon resonance effect of spherical shape gold nanoparticles present in the hydrogel matrix [28]. Increase of itaconic acid ratio in the GIAE nanocomposite hydrogels composition, the gold nanoparticles loading probably increased which in turn progressively increases the absorption in the UV–vis spectra. In all the UV–vis spectra of GIAE nanocomposite hydrogels

the characteristic peak appeared ~ 531, 529 and 536 nm, indicating the complete absence of gold nanoparticles aggregation. From the UV–vis spectral analysis of GIAE, it is very clear that the gold nanoparticles have incorporated in the hydrogel network [29, 30].

### 3.6 EDX studies of GIAE gold nanocomposite hydrogels

The results of energy dispersive X-ray analysis of gold nanoparticles shown in Fig. 8. The GIAE nanocomposite hydrogels showed an optical absorption band peak at ~ 2.0 keV, which is the typical absorption of metallic

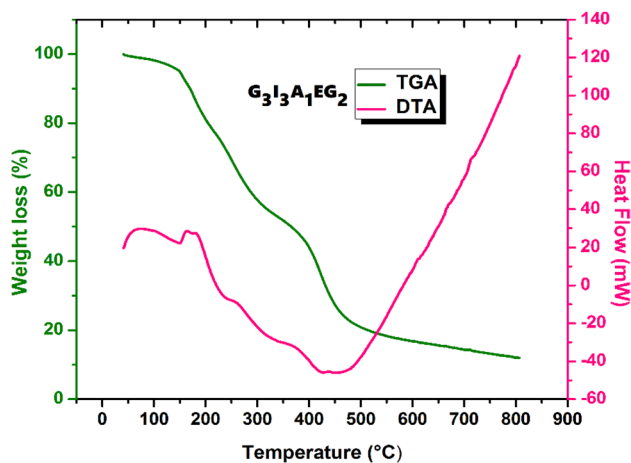


Fig. 6 TGA-DTA thermogram of  $G_3I_3A_1EG_2$  nanocomposite hydrogel

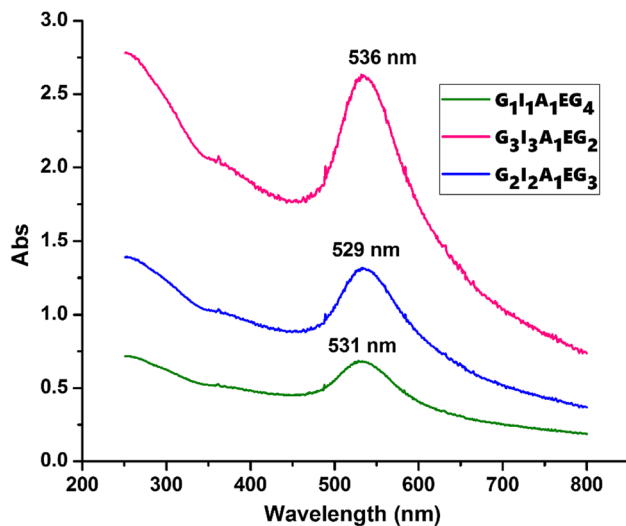


Fig. 7 UV-visible spectra of  $G_1I_1A_1EG_4$ ,  $G_2I_2A_1EG_3$  and  $G_3I_3A_1EG_2$  gold nanocomposite hydrogels

gold nanoparticles [31]. The scanned electron micrograph image of GIAE nanocomposite hydrogels showed an extreme distribution of gold nanoparticles within the hydrogel matrix. The  $G_1I_1A_1EG_4$  hydrogel found to be 0.72 weight % of gold nanoparticles composition. Similarly, the  $G_2I_2A_1EG_3$  and  $G_3I_3A_1EG_2$  nanocomposite hydrogels found to have 1.55%, 10.03% respectively. The plot of GIAE gold nanocomposite hydrogels demonstrated in the presence of carbon (C), oxygen (O) and gold (Au). These elements might have been present due to polymeric backbone possesses itaconic acid, acrylic acid, ethylene glycol and the gold nano solution. The weight percentage of gold composition of varied from  $G_1I_1A_1EG_4$  hydrogel to  $G_3I_3A_1EG_2$  hydrogel (0.72–10.03%) according to the amount of gold nano colloidal solution added during preparation. The EDX

quantitative analysis confirmed that the elemental composition of the Au nanoparticles in GIAE nanocomposite hydrogels [32].

### 3.7 TEM analysis of GIAE gold nanocomposite hydrogels

Figure 9 shows that transmission electron micrographs of gold nanoparticles morphology in GIAE nanocomposite hydrogels. The TEM image proves a uniform distribution of gold nanoparticles within the hydrogel matrix. It can be seen that gold nanoparticles were predominantly spherical in shape with sizes 5.64–36.12 nm. The obtained TEM images clearly shown that no agglomeration was formed during preparation of nanocomposites. According to Afzal et al. [33], it is clear that, the Au nanoparticles exhibit difference in morphology due to Au nano colloidal solution were added at different ratios during preparation of GIAE nanocomposite hydrogels.

### 3.8 Antibacterial activity of GIAE gold nanocomposite hydrogels

The GIAE gold nanocomposite hydrogels were subjected to antibacterial pathogens such as *Staphylococcus aureus* (gram + ve), *Bacillus cereus* (gram + ve) and *Escherichia coli* (gram – ve) and the results have shown in Fig. 10. The *Gentamicin* was chosen as a positive control with concentration of 500  $\mu\text{g}/\text{well}$ . The Antibacterial activity of GIAE gold nanocomposite hydrogels have been tested into 150, 300, 450 and 600  $\mu\text{g}$  concentrations. The  $G_1I_1A_1EG_4$  gold nanocomposite hydrogel showed zone of inhibition against *S. aureus* was 25, 30, 32, 34 mm and 21 mm for positive control. The inhibition zone against *E. coli* was about 10, 14, 21, 23 mm and 20 mm for positive control. The zone of inhibition against *B. cereus* was 21, 25, 27, 29 mm and 19 mm for positive control respectively. The obtained results revealed that the,  $G_1I_1A_1EG_4$  nanocomposite hydrogel have exhibited better zone of inhibition activity towards *S. aureus* and *B. cereus* than the *E. coli*. Conversely, The  $G_2I_2A_1EG_3$  nanocomposite hydrogel showed inhibition zone against *S. aureus* was about 16, 20, 25, 28 mm and 17 mm for positive control. The inhibition against *E. coli* was listed as 14, 17, 20, 23 mm and 21 mm for *gentamicin*. For *B. cereus* was about 18, 24, 28, 30 mm and 20 mm for (+ve) control. Similarly, the  $G_3I_3A_1EG_2$  nanocomposite hydrogel has shown zone of inhibition against *B. cereus* as 13, 15, 17, 23 mm and 29 mm for positive control. *E. coli* found to have 12, 14, 17, 22 mm and 27 mm towards *gentamicin*. For *S. aureus* showed 12, 13, 16 and 19 mm. The  $G_3I_3A_1EG_2$  have shown 24 mm for positive control. The antibacterial results

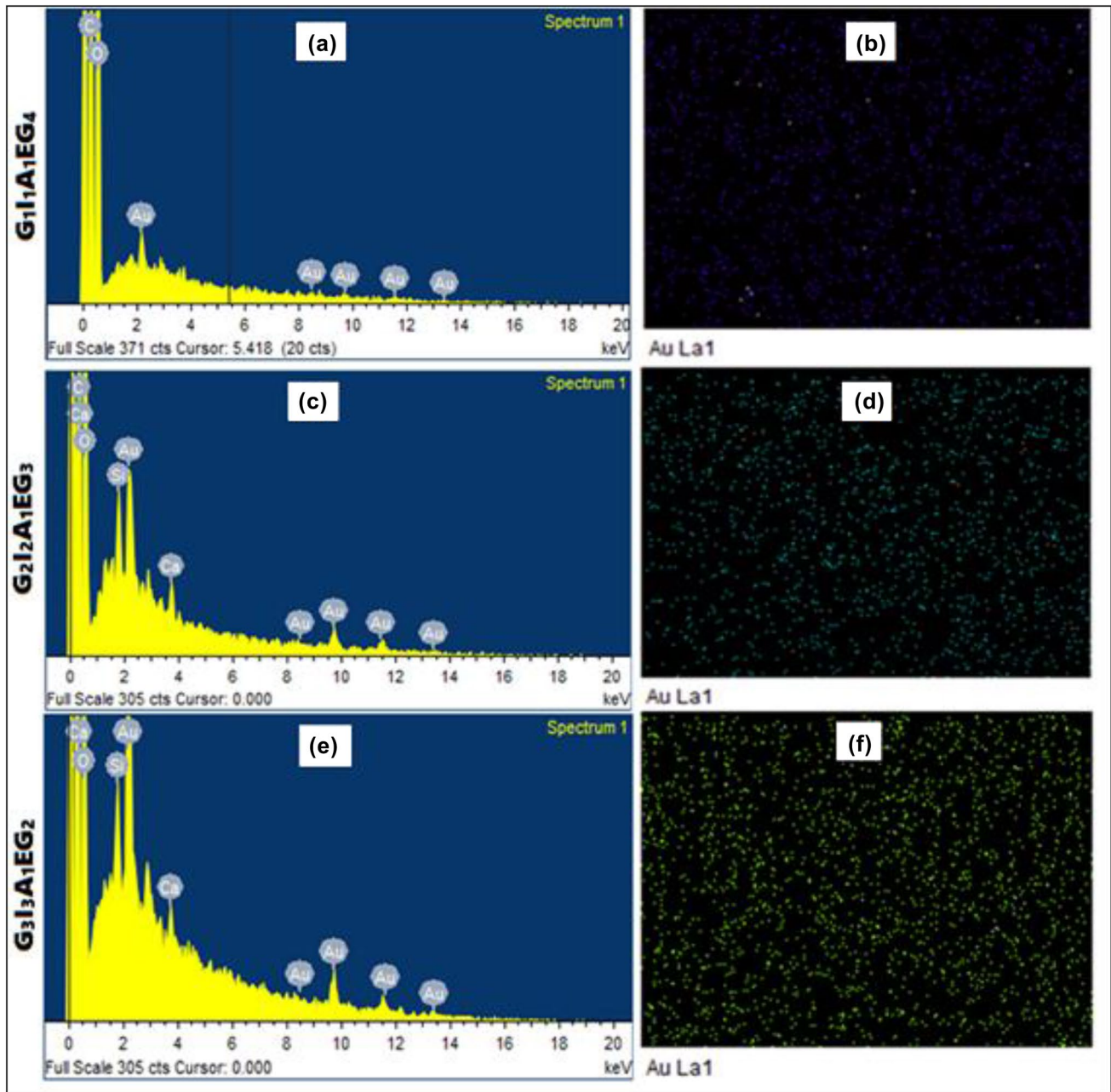


**Fig. 8** EDX spectrum and distribution of gold nanoparticles of  $G_{1I_1A_1EG_4}$  (a, b)  $G_{2I_2A_1EG_3}$  (c, d) and  $G_{3I_3A_1EG_2}$  (e, f) gold nanocomposite hydrogels

shown that the GIAE based nanocomposite hydrogels have shown good zone of inhibition towards all the three bacterial pathogens. Particularly, against *B. cereus* and *S. aureus* because the prepared hydrogel is anionic in nature. Hence, they showed highest zone of inhibition towards positive pathogens. Furthermore, the Au nanoparticles may interact with the surface of the cell membrane and disturbing respiratory function of the cell resulting in the death of bacterial pathogens [34].

### 3.9 Antifungal activity of GIAE gold nanocomposite hydrogels

The anti-fungal activities of GIAE nano composite hydrogels have shown in Fig. 11. The antifungal activity was examined against two pathogens such as *Aspergillus niger* and *Candida albicans*. The *ketoconazole* (100  $\mu\text{g}/\text{well}$ ) was used as a positive control. The antifungal activity of GIAE nanocomposite hydrogels has been found for different concentrations such as 15, 30, 45 and 60  $\mu\text{l}$  per well. The  $G_{1I_1A_1EG_4}$

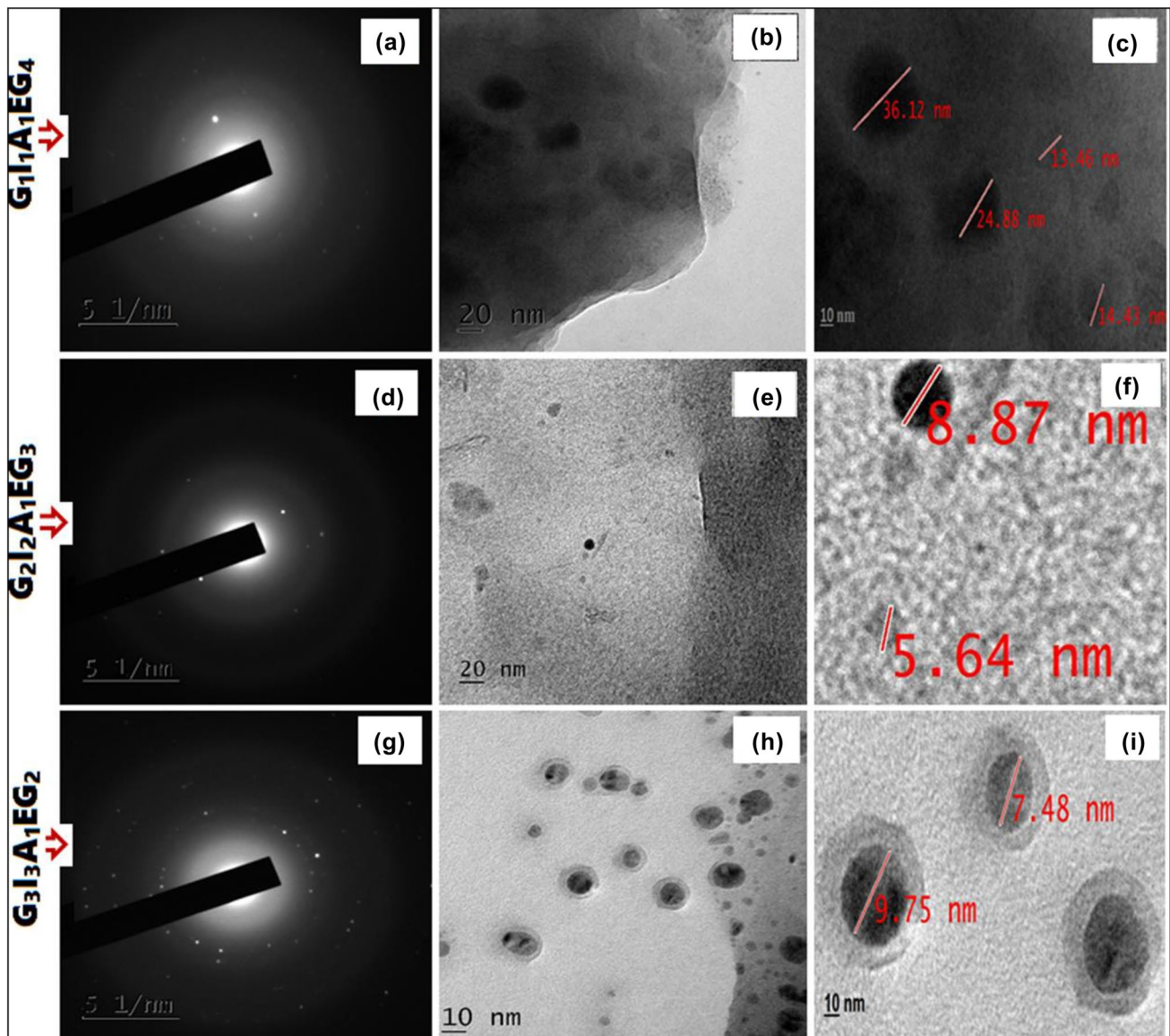


**Fig. 9** Electron diffraction pattern and TEM images of  $G_1I_1A_1EG_4$  (a–c)  $G_2I_2A_1EG_3$  (d–f) and  $G_3I_3A_1EG_2$  (g–i) gold nanocomposite hydrogels

nanocomposite hydrogel showed zone of inhibition against *A. niger* was 9, 11, 13, 15 mm and 26 mm for positive control. Similarly, against *C. albicans* was 0, 15, 17, 20 mm and 40 mm for *ketoconazole*. Moreover, the  $G_2I_2A_1EG_3$  nanocomposite hydrogel has shown zone of inhibition towards *A. niger* as 13, 15, 19, 22 mm and for positive control 11 mm. Likewise, *C. albicans* found to have 0, 20, 25, 30 mm and 22 mm for positive control. In order to  $G_3I_3A_1EG_2$  nanocomposite hydrogel, the *A. niger* was 14, 16, 19, 22 mm and 23 mm for positive control. The *C. albicans* found to be 11, 14, 16, 19 mm and 28 mm for positive control respectively. The anti-fungal zone revealed that the prepared GIAE based nanocomposite hydrogels have shown good efficacy towards pathogens. Since, among the prepared GIAE based nanocomposite

hydrogels, the  $G_3I_3A_1EG_2$  showed highest zone of inhibition than the  $G_1I_1A_1EG_4$ ,  $G_2I_2A_1EG_3$  nanocomposite hydrogels. Due to, it possesses high concentration of gold nanoparticles and itaconic acid. In general, gold nanoparticles have increased in surface area hence, they may easily diffuse through the cell membrane to the inside of the cell. Therefore, cell retards their normal functioning like replication and finally to the cell death [35, 36].

### 3.10 Cytotoxicity studies of GIAE gold nanocomposite hydrogels

The microscopic images and % of cell viability for GIAE based nanocomposite hydrogels have shown in Fig. 12

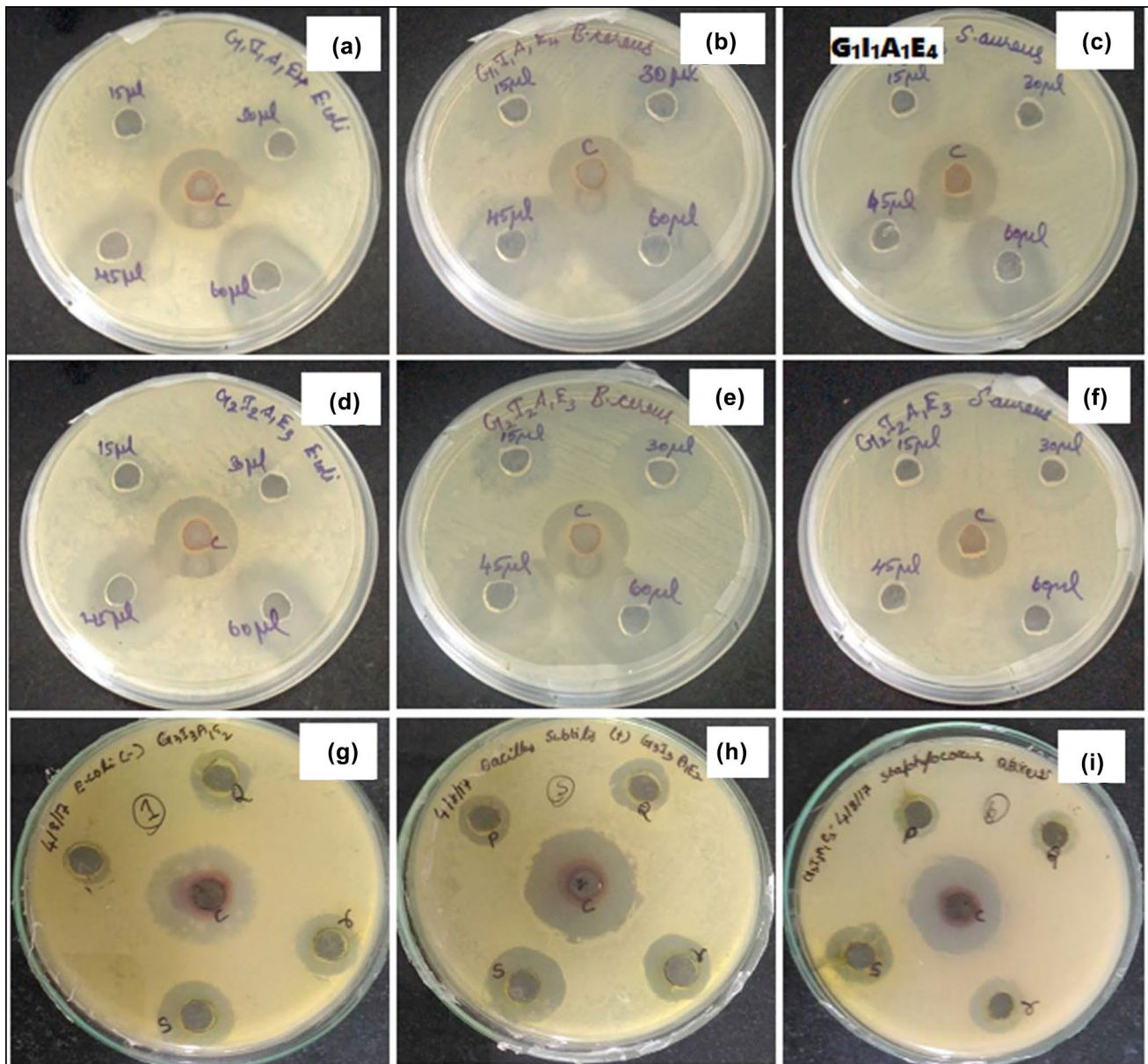


**Fig. 10** Anti-bacterial activity of  $G_{1I_1A_1}EG_4$  (a–c)  $G_{2I_2A_1}EG_3$  (d–f) and  $G_{3I_3A_1}EG_2$  (g–i) gold nanocomposite hydrogels

and Table 2. In utilizing  $G_{1I_1A_1}EG_4$  nanocomposite hydrogel the cell viability % was about 92% with 10  $\mu\text{g}/\text{mL}$  and 90% for 250  $\mu\text{g}/\text{mL}$ . Likewise, the  $G_{2I_2A_1}EG_3$  showed 101% cell proliferation with 10  $\mu\text{g}/\text{mL}$  and 89% for 250  $\mu\text{g}/\text{mL}$ . The  $G_{3I_3A_1}EG_2$  gold nanocomposite hydrogel exhibited cell proliferation for 10  $\mu\text{g}/\text{mL}$  was 109% and 93% for 250  $\mu\text{g}/\text{mL}$  respectively. The prepared GIAE nanocomposite hydrogels showed cell viability against control was 100%. The obtained cytotoxicity results revealed that the prepared GIAE nanocomposite hydrogels were possessed ~90% of proliferation towards 3T3 fibroblast cell lines. Conversely, if any extract causes the destruction of 50% of the cell population, IC 50(%) is known as the cytotoxic

index. Henceforth, none of the prepared nanocomposite hydrogels were toxic in nature. The  $G_{3I_3A_1}EG_2$  nanocomposite hydrogel exhibited highest cell viability % than the  $G_{1I_1A_1}EG_4$ ,  $G_{2I_2A_1}EG_3$  nanocomposites. It is due to the composition of itaconic acid and gold nanoparticles. Since, the gold nanoparticles are inert in nature, acute cytotoxicity has not been observed so far [37].

### 3.11 Degradation studies of GIAE gold nanocomposite hydrogels

The degradation studies of GIAE based nanocomposite hydrogels have carried out by weight loss method in

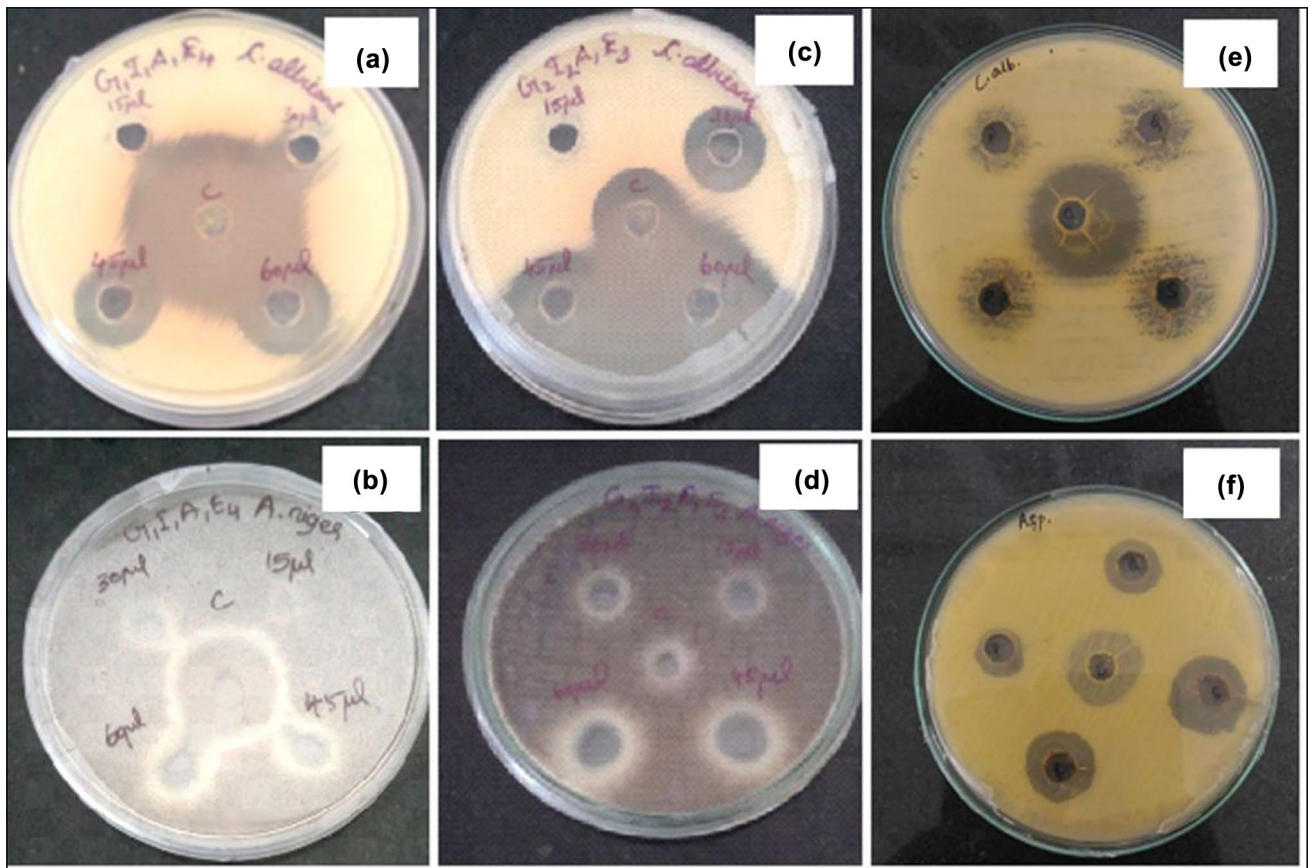


Fig. 11 Antifungal activity of  $G_{11}I_1A_1EG_4$  (a, b),  $G_{21}I_2A_1EG_3$  (c, d) and  $G_{31}I_3A_1EG_2$  (e, f) gold nanocomposite hydrogels

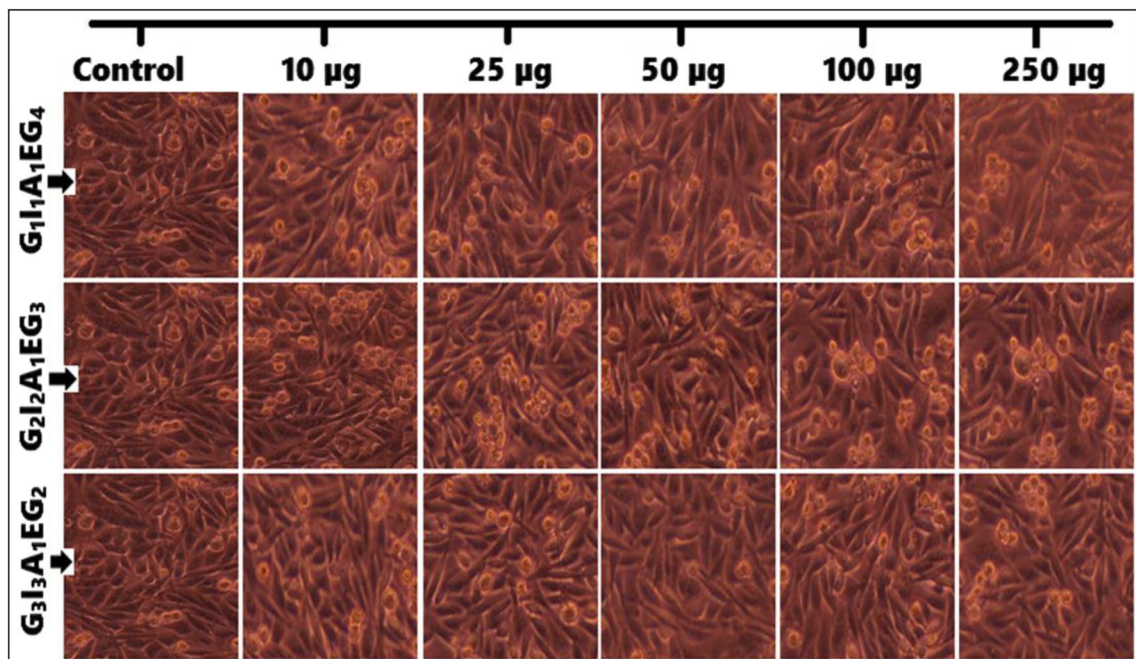


Fig. 12 Microscopic images of 3T3 fibroblast cell lines treated with  $G_{11}I_1A_1EG_4$ ,  $G_{21}I_2A_1EG_3$  and  $G_{31}I_3A_1EG_2$  gold nanocomposite hydrogels with respect to concentration

**Table 2** The cell viability % of GIAE nanocomposite hydrogels with respect to concentration

S. no	Sample concentration ( $\mu\text{g/mL}$ )	Cell viability (%)		
		$G_1I_1A_1EG_4$	$G_2I_2A_1EG_3$	$G_3I_3A_1EG_2$
1	10	92	101	109
2	25	99	90	97
3	50	96	96	99
4	100	95	93	98
5	250	90	89	93
6	Control	100	100	100

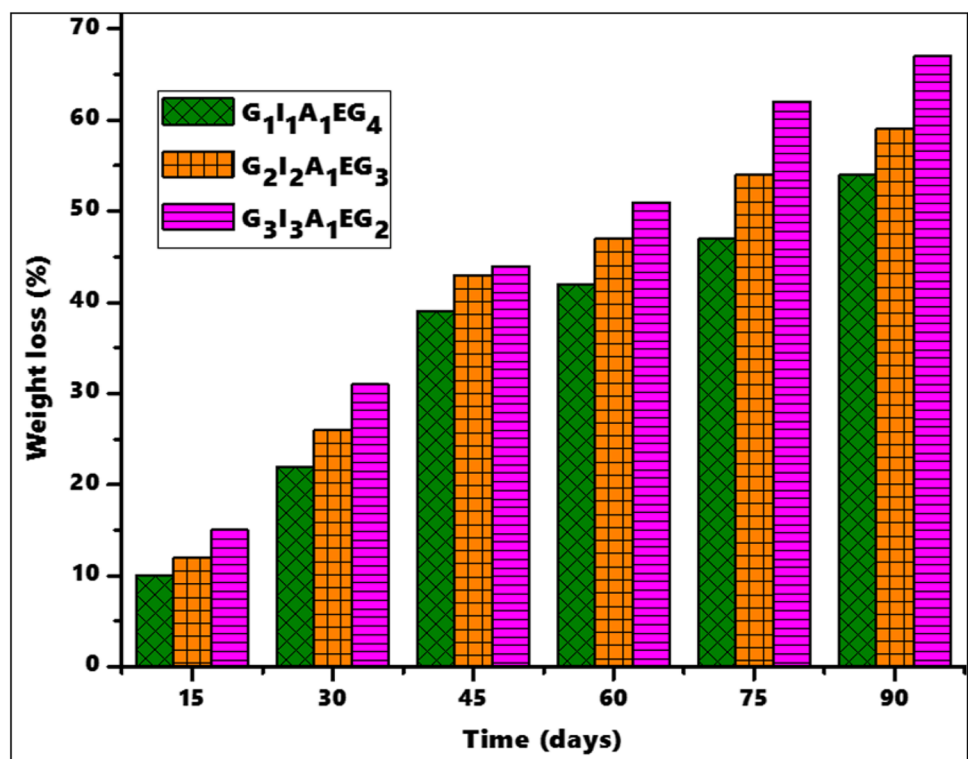
the period of 90 days. The obtained weight loss (%) of GIAE nanocomposite hydrogels have shown in Fig. 13. The results of degradation was found that the  $G_1I_1A_1EG_4$  nanocomposite hydrogel showed ~54% of weight loss. However, the  $G_2I_2A_1EG_3$  nanocomposite hydrogel underwent ~59% of degraded weight loss. In the meantime, the  $G_3I_3A_1EG_2$  unveiled a ~67% of weight loss. It was found that the nanocomposite hydrogels showed lesser degraded weight loss than the polymeric hydrogel [38]. It might be on the basis of gold nanoparticles. Likewise, during degradation the gold nanoparticles escape from the polymeric backbone in aqueous medium and may attach to the bacterial cell wall and rupture it, which causes leakage of intracellular substances and eventually causes cell death. On the other hand, the gold nanoparticles can also

penetrate into the cells and adversely affect the cellular metabolic activities of bacteria and eventually death of the microbe. In general, gold nanoparticles are capable of causing a bacteriostatic (growth inhibition) effect. Therefore, the degradation percentage of nanocomposites have been decreased for  $G_1I_1A_1EG_4$ ,  $G_2I_2A_1EG_3$  nanocomposite hydrogels than the  $G_3I_3A_1EG_2$  due to the composition of itaconic acid and gold nanoparticles [39].

## 4 Conclusions

- In summary, a series of GIAE gold nanocomposite hydrogels have been prepared viz. greener approach. The preparation methodology was comparatively gorgeous than the other method of formulation. This preparation method had been yet unreported in the literatures.
- The prepared itaconic acid based GIAE gold nanocomposite hydrogels have revealed the maximum extent of swelling at pH 7.4–10 due to the formation of carboxylate anion. As a result, obtained nanocomposite may utilize in biomedical applications because, many of the body fluids have neutral pH conditions.
- The results of thermal studies conclude that gold nanocomposite hydrogels were good thermal stability due to impact of gold nanoparticles.

**Fig. 13** The degradable weight loss percentage of  $G_1I_1A_1EG_4$ ,  $G_2I_2A_1EG_3$  and  $G_3I_3A_1EG_2$  gold nanocomposite hydrogels



- The elemental composition of incorporation of gold nanoparticles in gold nanocomposite hydrogels were elucidated by Energy Dispersive X-ray (EDX) microanalysis technique. The obtained spectrum results confirmed that the presence of a strong elemental absorption peak for gold at ~ 2 keV.
  - The size of gold nanoparticles played an important key role to determine the properties of gold nanocomposite hydrogels, it might be to large surface area of gold particles.
  - The antimicrobial zone of inhibition owing to the concentration and size of gold nanoparticles. In general, smaller gold nanoparticles can easily interact with the cell wall of pathogens. It's leading to retard their normal functioning and finally to the cell disintegration.
  - The GIAE showed more than 90% of cell viability index. It is due to the stoichiometric amount of itaconic acid and gold nanoparticles.
  - The obtained nanocomposite hydrogels underwent 67% of degradation it might be in the formation of ester moieties in polymerization which facilitated the quick degradation process.
  - Since, all above aspects revealed the GIAE gold nanocomposite hydrogels are eco-friendly, nontoxic and soft matter. Henceforth, it may be accentuated for biomedical applications.
7. Tibbitt MW, Anseth KS (2009) Hydrogels as extracellular matrix mimics for 3D cell culture. *Biotechnol Bioeng* 103:655–663
  8. Goenka S, Sant V, Sant S (2014) Graphene-based nanomaterials for drug delivery and tissue engineering. *J Control Release* 173:75–88
  9. Peppas NA, Hilt JZ, Kadeem Hosseini A et al (2006) Hydrogels in biology and medicine: from molecular principles to bio nanotechnology. *Adv Mater* 18:1345–1360
  10. Wang E, Desai MS, Lee SW (2013) Light-controlled graphene-elastin composite hydrogel actuators. *Nano Lett* 13:2826–2830
  11. Thomas V, Mohan YM, Sreedhar B (2007) Versatile strategy to fabricate hydrogel–silver nanocomposites and investigation of their antimicrobial activity. *J Colloid Interfaces Sci* 315:389–395
  12. Bal A, Cepni FE, Çakir O et al (2015) Synthesis and characterization of copolymeric and terpolymeric hydrogel–silver nanocomposites based on acrylic acid, acrylamide and itaconic acid: investigation of their antibacterial activity against gram-negative bacteria. *Braz J Chem Eng* 32:509–518
  13. Tibbitt MW, Anseth KS (2009) Hydrogels as extracellular matrix mimics for 3D cell culture. *Biotechnol Bioeng* 103:655–663
  14. McCrory R, Jones DS, Adair CG (2003) Pharmaceutical strategies to prevent ventilator-associated pneumonia. *J Pharm Pharmacol* 55:411–428
  15. Killion JA, Geever LM, Devine DM et al (2014) Compressive strength and bioactivity properties of photopolymerizable hybrid composite hydrogels for bone tissue engineering. *Int J Polym Mater* 63:641–650
  16. Guzman M, Dille J, Stephane G (2012) Synthesis and antibacterial activity of silver nanoparticles against Gram-positive and Gram-negative bacteria. *Nanomedicine* 8:37–45
  17. Bojana O, Jasmina S, Zeljka J et al (2012) Novel alginate based nanocomposite hydrogels with incorporated silver nanoparticles. *J Mater Sci Mater Med* 23:99–107
  18. Jayaramudua T, Raghavendra GM, Varaprasad K et al (2013) Development of novel biodegradable Au nanocomposite hydrogels based on wheat: for inactivation of bacteria. *Carbohydr Polym* 92:2193–2200
  19. Raghavendra GM, Jayaramudua T, Varaprasad K et al (2015) Antibacterial nanocomposite hydrogels for superior biomedical applications: a facile eco-friendly approach. *RSC Adv* 5:14351–14358
  20. Sakthivel M, Franklin DS, Guhanathan S (2016) pH-sensitive Itaconic acid based polymeric hydrogels for dye removal applications. *Ecotoxicol Environ Saf* 134:427–432
  21. Xiang Y, Chen D (2007) Preparation of a novel pH-responsive silver nanoparticle/poly(HEMA–PEGMA–MAA) composite hydrogel. *Eur Polym J* 10:4178–4187
  22. Sakthivel M, Franklin DS, Sudarsan S et al (2017) Investigation on pH/salt-responsive multifunctional itaconic acid based polymeric biocompatible, antimicrobial and biodegradable hydrogels. *React Funct Polym* 122:9–21
  23. Li B, Jiang Y, Liu Y et al (2009) Novel poly(Nisopropylacrylamide)/clay/poly(acrylamide) IPN hydrogels with the response rate and drug release controlled by clay content. *J Polym Sci Phys* 47:96–106
  24. Mahdavinia GR, Pourjavadi A, Hosseinzadeh H et al (2004) Superabsorbent hydrogels from poly(acrylic acid-co-acrylamide) grafted chitosan with salt- and pH-responsiveness properties. *Eur Polym J* 40:1399–1407
  25. Varaprasad K, Ravindra S, Narayana Reddy N et al (2010) Design and development of temperature sensitive porous poly(NIPAAm-AMPS) hydrogels for drug release of doxorubicin-a cancer chemotherapy drug. *J Appl Polym Sci* 116:3593–3602
  26. Ranga Reddy P, Varaprasad K, Narayana Reddy N et al (2012) Fabrication of Au and Ag Bi-metallic nanocomposite for antimicrobial applications. *J Appl Polym Sci* 2012:1357–1362

## Compliance with ethical standards

**Conflict of interest** On behalf of all authors, the corresponding author states that there is no conflict of interest.

## References

1. Helvacioğlu E, Aydın V, Nugay T et al (2011) High strength poly(acrylamide)-clay hydrogels. *J Polym Res* 18:2341–2350
2. Matsumoto M, Yoshida R, Kataoka K (2004) Glucose-responsive polymer gel bearing phenylborate derivative as a glucose-sensing moiety operating at the physiological pH. *Biomacromolecules* 5:1038–1045
3. Gaharwar AK, Peppas N, Khademhosseini A (2014) Nanocomposite hydrogels for biomedical applications. *Biotechnol Bioeng* 111:441–453
4. Sharma G, Thakur B, Naushad M et al (2018) Applications of nanocomposite hydrogels for biomedical engineering and environmental protection. *Environ Chem Lett*. <https://doi.org/10.1007/s10311-017-0671-x>
5. Yu Y, Li Y, Liu L et al (2011) Synthesis and characterization of pH and thermoresponsive poly(N-isopropylacrylamide-co-itaconic acid) hydrogels crosslinked with N-maleyl chitosan. *J Polym Res* 18:283–291
6. Discher DE, Mooney DJ, Zandstra PW (2009) Growth factors, matrices, and forces combine and control stem cells. *Science* 324:1673–1677

27. Afzal AB, Javed Akhtar M, Nadeem M et al (2009) Investigation of structural and electrical properties of polyaniline/gold nanocomposites. *J Phys Chem C* 113:17560–17565
28. Frens G (1973) Controlled nucleation for the regulation of the particle size in monodisperse gold suspensions. *Nature-Phys Sci* 241:20–22
29. Liu FK, Hsieh SY, Ko FH et al (2003) Synthesis of nanometer-sized poly (methyl methacrylate) polymer network by gold nanoparticle template. *Jpn J Appl Phys* 42:4147–4151
30. Turkevich J, Stevenson PC, Hillier J (1951) A study of the nucleation and growth processes in the synthesis of colloidal gold. *Discuss Faraday Soc* 11:55–75
31. Elavazhagan T, Arunachalam KD (2011) Memecylon edule leaf extract mediated green synthesis of silver and gold nanoparticles. *Int J Nanomed* 6:1265–1278
32. Wim H, Jong D, Burger MC et al (2010) Detection of the presence of gold nanoparticles in organs by transmission electron microscopy. *Materials* 3:4681–4694
33. Afzal AB, Javed Akhtar M, Nadeem M et al (2009) Investigation of structural and electrical properties of polyaniline/gold nanocomposites. *J Phys Chem C* 113:17560–17565
34. Pal S, Tak YK, Song JM (2007) Does the antibacterial activity of silver nanoparticles depend on the shape of the nanoparticles? A study of the gram-negative bacterium *Escherichia coli*. *Appl Environ Microbiol* 73:1712–1720
35. Ahmad T, Wani IA, Lone IH et al (2013) Antifungal activity of gold nanoparticles prepared by solvothermal method. *Mater Res Bull* 1:12–20
36. Tan YN, Lee KH, Su X (2011) Study of single-stranded DNA binding protein-nucleic acids interactions using unmodified gold nanoparticles and its application for detection of single nucleotide polymorphisms. *Anal Chem* 83:4251–4257
37. Connor EE, Mwamuka J, Gole A et al (2005) Gold nanoparticles are taken up by human cells but do not cause acute cytotoxicity. *Small* 1:325–327
38. Sakthivel M, Franklin DS, Sudarsan S et al (2016) Investigation on pH-switchable (itaconic acid/ethylene glycol/acrylic acid) based polymeric biocompatible hydrogel. *RSC Adv* 6:106821–106831
39. Sun C, Qu R, Chen H et al (2008) Degradation behavior of chitosan chains in the green synthesis of gold nanoparticles. *Carbohydr Res* 15:2595–2599